Zn(II)porphyrin Helical Arrays: A Strategy to Overcome Conformational Heterogeneity by Host-Guest Chemistry

Zin Seok Yoon, Shanmugam Easwaramoorthi, and Dongho Kim*

Center for Ultrafast Optical Characteristics Control and Department of Chemistry, Yonsei University, Seoul 120-749, Korea
**E-mail: dongho@yonsei.ac.kr*
Received November 20, 2007

Conformational heterogeneity of directly linked multiporphyrin arrays with larger molecular length retards their utilities in practical applications such as two-photon absorption and molecular photonic wire. In this regard, here we adopted a way to overcome the conformational heterogeneity through hydrogen bonding by selective binding of meso aryl substituents of porphyrins (host) with urea (guest) to form helical structure. Using steady-state and time-resolved spectroscopy, we observed the enhanced fluorescence quantum yield by ~1.8 to 2.4 times, enhanced anisotropy values and the disappearance of fast fluorescence decay component in the host-guest helical forms. In addition, the enhanced nonlinear optical responses of helical arrays infer the extended inter-porphyrin electronic coupling due to a significant change in dihedral angle between the neighboring porphyrin moieties. The current host-guest strategy will provide a guideline to improve the structural homogeneity of the photonic wire.

Key Words : Zn(II)porphyrin arrays, Conformational heterogeneity, Two-photon absorption, Host-guest binding, Fluorescence quantum yield

Introduction

Recently, various multiporphyrin arrays have been fabricated for applications in molecular photonic devices.[1-5] These porphyrinoid block copolymer systems have shown many advantages in manipulating photophysical properties through modification of peripheral substitutions at meso and beta carbons with desirable functional groups, complexation ability with different metals, and assembling porphyrin monomers *via* covalent and noncovalent bonds. Among many candidates, covalently linked orthogonal Zn(II)porphyrin arrays (**Z*N***, *N* is the number of porphyrin monomers) have been regarded to be promising materials as molecular wire due to the strong interactions between the adjacent porphyrin units.[6-9] However, after the synthesis of **Z*N***, unfortunately, some evidences of "conformational heterogeneity", a negative factor in manufacturing molecular devices was revealed, based on spectroscopic and microscopic measurements in bulk solution, single-molecule fluorescence analysis, and STM (scanning tunneling microscope) images.[10-12] As the meso-meso directly linked porphyrin arrays become longer than 16 units, the longer arrays (***Z24***, ***Z32***, and so on, up to ***Z1024***) showed reduced fluorescence quantum yields and fluorescence excitation anisotropy values, and increased nonradiative decay channels in the excited states. These photophysical features have been considered as serious drawbacks for their practical applications as molecular wires, because a homogeneous conformation of molecules should be suitable for connecting source and drain electrode junctions, and transporting charge carriers or photons effectively. Thus, it is indispensable to overcome the conformational heterogeneity in linear porphyrin arrays, preserving straight molecular shape, in order to utilize them for nano-sized molecular wires.

In this regard, here we have introduced a way to overcome the conformational heterogeneity by selective binding of host, porphyrin array and guest, cyclic urea moieties by using hydrogen bonding to form helical arrays.[13] Based on the following experiments including steady-state absorption and emission, and time resolved fluorescence spectroscopy as well, we could provide some evidences on the improved conformational homogeneity. By reducing the conformational heterogeneity, the formation of helical arrays has also allowed the enhanced nonlinear optical response probed by femtosecond *Z*-scan technique.[14]

Experimental

Synthesis. The synthetic details of ZNH arrays and guest molecules are described elsewhere.[13]

Steady-state Absorption and Emission Spectra. Steady-state absorption spectra were acquired using an UV-VIS-NIR spectrometer (Varian, Cary5000). Steady-state fluorescence spectra were recorded on a fluorescence spectrometer (Hitachi, FL2500). For the observation of near-infrared (NIR) emission spectra, a photomultiplier (Hamamatsu, R5108), a lock-in amplifier (EG&G 5210), combined with a chopper after laser excitation at 442 nm from a CW He-Cd laser (Melles Griot, Omnichrome 74) were used.

Time-correlated Single Photon Counting. Time-resolved fluorescence was detected using a time-correlated single-photon-counting (TCSPC) technique. A home-made cavity dumped Ti:Sapphire oscillator pumped by a CW Nd:YVO4 laser (Coherent, Verdi) was used as the excitation light source; this provided ultrashort pulses (100 fs at full width half maximum) and allowed for a high repetition rate (200-

400 kHz). The output pulse of the oscillator was frequency-doubled with a second harmonic crystal. The TCSPC detection system consisted of a multichannel plate photomultiplier (Hamamatsu, R3809U-51) with a cooler (Hamamatsu, C4878), a TAC (time-to-amplitude converter) (EG&G Ortec, 457), two discriminators (EG&G Ortec, 584 (signal) and Canberra, 2126 (trigger)), and two wideband amplifiers (Philip Scientific (signal) and a Mini Circuit (trigger)). A personal computer with a multichannel analyzer (Canberra, PCA3) was used for data storage and processing. The overall instrumental response function was about 60 ps (fwhm). A sheet polarizer, set at an angle complementary to the magic angle (54.7), was placed in the fluorescence collection system. The decay fittings were determined using a least-squares deconvolution process (LIFETIME program with an iterative nonlinear least-squares deconvolution procedure developed at the University of Pennsylvania).[11]

Open-aperture Femtosecond Z-scan. The TPA experiments were performed using the open-aperture Z-scan method with 130 fs pulses from an optical parametric amplifier (Light Conversion, TOPAS) operating at a 5 kHz repetition rate using a Ti:sapphire regenerative amplifier system (Spectra-Physics, Hurricane). The laser beam was divided into two parts. One was monitored by a Ge/PN photodiode (New Focus) as intensity reference, and the other was used for the transmittance studies. After passing through an f = 10 cm lens, the laser beam was focused and passed through a quartz cell. The position of the sample cell could be varied along the laser-beam direction (z-axis), so the local power density within the sample cell could be changed under a constant laser power level. The thickness of the cell was 1 mm. The transmitted laser beam from the sample cell was then probed using the same photodiode as used for reference monitoring. The on-axis peak intensity of the incident pulses at the focal point, I_0, ranged from 40 to 60 GW/cm. Assuming a Gaussian beam profile, the nonlinear absorption coefficient β can be obtained by curve fitting to the observed open aperture traces with the following equation:

$$T(z) = \frac{\beta I_0 (1 - e^{-\alpha_0 l})}{2\alpha_0 (1 + (z/z_0)^2)}.$$

where α_0 is the linear absorption coefficient, l the sample length, and Z_0 the diffraction length of the incident beam. After obtaining the nonlinear absorption coefficient β, the TPA cross-section $\sigma^{(2)}$ (in units of 1 GM = 10^{-50} cm^4·s/photon·molecule) of a single solute molecule sample can be determined by using the following relationship:

$$\beta = \frac{\delta N_A d \times 10^{-3}}{h\nu},$$

where N_A is the Avogadro constant, d the concentration of the TPA compound in solution, h the Planck's constant, and υ is the frequency of the incident laser beam. So as to satisfy the condition of $\alpha_0 l << 1$, which allows the pure TPA $\sigma^{(2)}$ values to be determined using a simulation procedure, the TPA cross-section value of AF-50 was measured as a reference compound; this control was found to exhibit a TPA value of 50 GM at 800 nm.

Results and Discussion

Figure 1 shows the steady-state absorption and fluore-

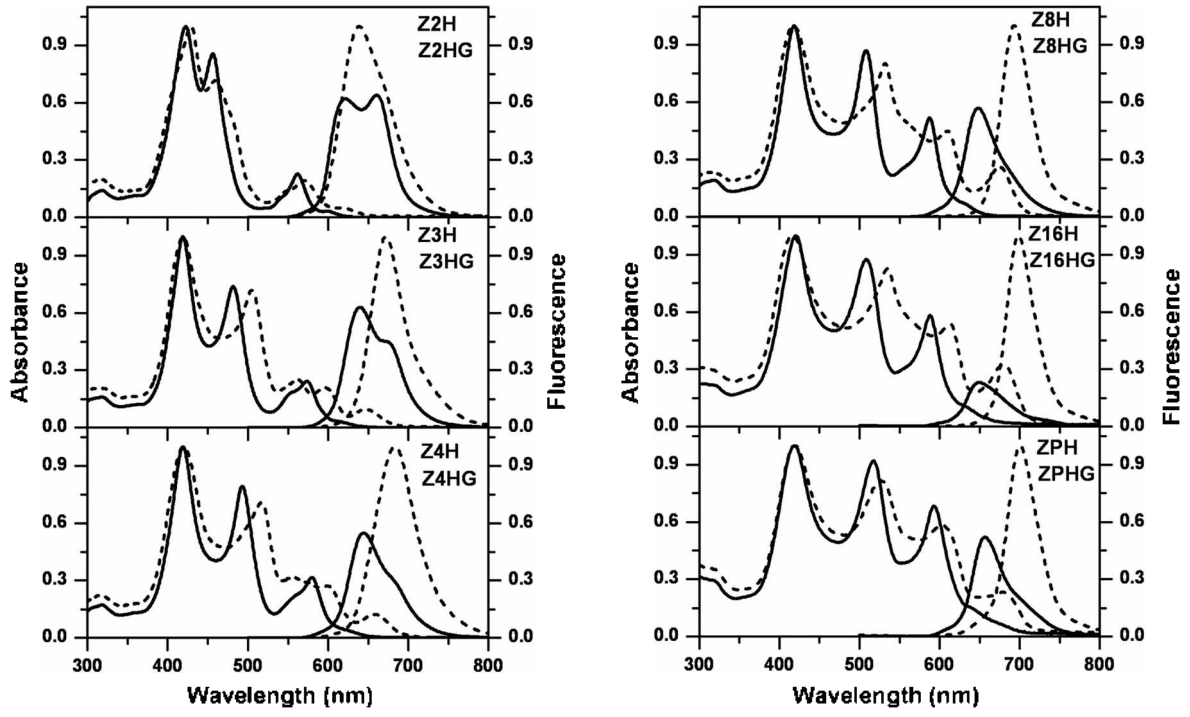

Figure 1. Steady-state absorption and emission spectra of **ZnH** and **ZnHG**.

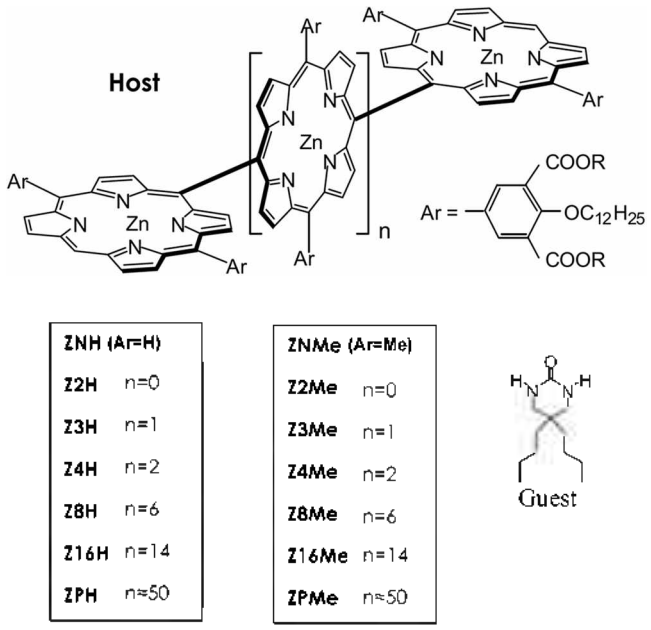

Scheme 1. Molecular structure of linear Zn(II)porphyrin arrays (host) and urea (guest).

scence spectra of a series of **Z*N*H** as depicted in Scheme 1 and **Z*N*HG** (**Z*N*H** with guest binding) in toluene/THF (9:1) solvent mixture. The splitting in Soret band is a characteristic feature of orthogonal Zn(II)porphyrin arrays, which reflects excitonic interaction between porphyrin monomer units.[11] In the presence of excess amount of guest molecules **Z*N*H** (*N* = 2, 3, 4, 8, 16, ~50) undergoes significant absorption spectral changes corresponding to the formation of **Z*N*HG** through hydrogen bonding. The **Z*N*HG** showed broad and red-shifted low-energy Soret bands around 500 nm, compared to **Z*N*H**, while the position of high-energy Soret bands remains unchanged. In addition, the lowest energy absorption bands were also red-shifted in **Z*N*HG** around 600-700 nm, followed by the mirror image fluorescence spectra, regardless of excitation wavelengths. These observed spectral changes can be explained by the increased inter-porphyrin electronic communication caused by the reduced dihedral angle between the neighboring porphyrin moieties due to hydrogen bonding. It should be noted that the fluorescence quantum yields (Φ_f) of **Z*N*HG** (Table 1) are in the range from 0.045 to 0.187, which are 1.8-2.4 times larger than those of **Z*N*H**. Especially, the Φ_f of **Z*16*HG** (0.187) is the highest value in zinc(II) porphyrin array systems. The very low Φ_f of **Z*N*H** arrays longer than 16 porphyrin units can be explained in terms of conformational heterogeneity,[11] seemingly resulting from the dihedral angle distribution between the porphyrin units. In reality, the dihedral angle distribution was estimated to be 90 ± 15° in **Z*2*H** by AM1 calculation. After the guest binding, **Z*N*H** forms rigid helical structure, thereby reduces the degree of dihedral angle distribution and results in an enhancement in the fluorescence quantum yield.

In relation to the broad absorption spectra in **Z*N*HG**, the helical formation of orthogonal arrays is considered to

Table 1. Photophysical properties of **Z*N*H** and **Z*N*HG** arrays.

Compounds	Φ_F[a]	r[b]	τ[c] (ns)	τ_0[d] (ns)	Φ_τ[e] (ns)	$\sigma^{(2)}$ (GM)[f]
Z*2*H	0.029	0.05	1.87	64.5	1.50	<100
Z*3*H	0.040	0.11	1.76	44.0	1.85	<100
Z*4*H	0.048	0.16	1.67	34.8	3.20	<100
Z*8*H	0.062	0.28	1.57	25.3	6.94	<100
Z*16*H	0.077	0.30	1.56	20.3	–	<100
Z*P*H	0.064	0.17	0.46	7.2	–	<100
Z*2*HG	0.045	0.07	1.87	41.6	1.72	4500
Z*3*HG	0.063	0.19	1.62	25.7	2.58	9600
Z*4*HG	0.087	0.23	1.60	18.4	3.56	11800
Z*8*HG	0.111	0.32	1.47	133.2	8.02	12800
Z*16*HG	0.187	0.32	1.20	6.4	–	13500
Z*P*HG	0.099	0.22	1.15	11.6	–	14700

[a]Fluorescence quantum yields (Φ_F). [b]Anisotropy values (r). [c]Averaged fluorescence decay lifetimes (τ). [d]Natural radiative decay rate constants (τ_0). [e]Rotational diffusion time constants (Φ). [f]Two-photon absorption cross section (σ).

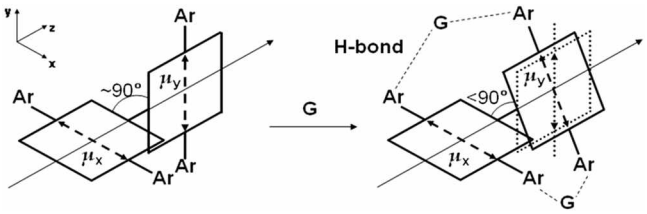

Scheme 2. Enhanced excitonic interaction induced by reduced dihedral angle in helical formation with in host-guest binding.

induce stronger excitonic interactions than **Z*N*H** through the formation of more rigid molecular structure as shown in Scheme 2. The noninteracting transition dipoles between monomers in **Z*N*H** by mutually orthogonal orientation of μ_x and μ_y make the orientation factor (κ) close to zero. However, as a result of reduced dihedral angle through guest binding, the orientation factor becomes nonzero value, which leads the interaction between transition dipoles, then further resulting in the broadening of absorption spectra.

In order to find out the relative orientation between absorption and emission transition dipoles, fluorescence excitation anisotropy (FEA) spectra were measured in **Z*N*H** and **Z*N*HG** in mixed solvents, monitored at the maxima of fluorescence spectra, as shown in Figure 2. In our previous report, we have observed the transition dipoles corresponding to fluorescence emission dipole in linear zinc(II) porphyrin arrays are oriented along the molecular z-axis.[4,11] Compared to the anisotropy values of **Z*N*H**, those of **Z*N*HG** are always higher in the entire wavelength region. One of the major factors affecting the anisotropy values can be the rotational diffusion in solution, so the current FEA values indicate the larger molecular hydrodynamic volume in **Z*N*HG** caused by the guest binding, resulting from the rigid and linear molecular structure.

The reduced nonradiative decay channels in helical arrays were confirmed by fluorescence lifetime measurement using time-correlated single photon counting (TCSPC). Figure 3

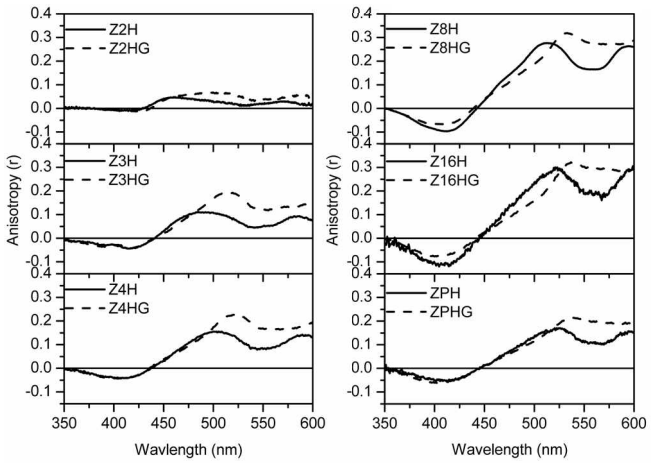

Figure 2. Steady-state fluorescence excitation anisotropy (FEA) spectra of **ZNH** and **ZNHG**.

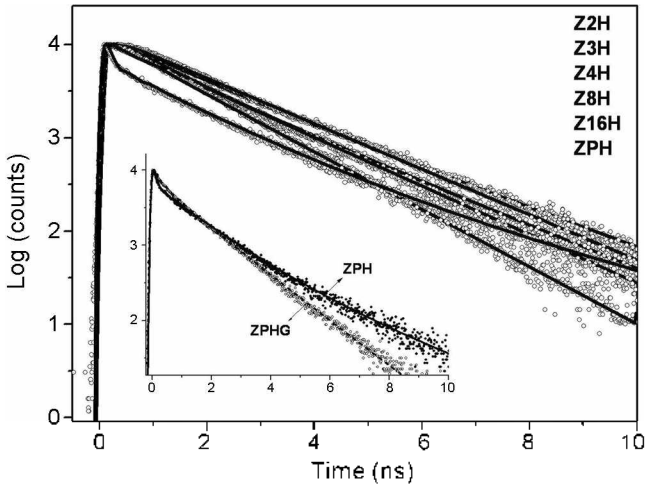

Figure 3. Singlet excited-state fluorescence decay profiles of **ZNH**. Inset shows a comparison of **ZPH** and **ZPHG**.

shows the fluorescence decay profiles of **ZNH** arrays and **ZPH**/**ZPHG** as inset, and the deconvolution fitting results are presented in Table 1. As the arrays become longer, the average fluorescence lifetimes of **ZNH** and **ZNHG** consistently become shorter. Meanwhile, the arrays >**Z*16*H** exhibits multiexponential decay in contrast with the single exponential decay in shorter arrays, where fast decay component (~100 ps) becomes manifest for **ZPH**, in addition to the slow decay component commonly seen in shorter arrays. We have assigned that the fast decay component of ~100 ps originates from conformational heterogeneity of longer arrays in our previous report. As the arrays become longer, the amplitudes of shorter decay components continuously increase, reflecting the higher degree of conformational heterogeneity in longer arrays.[11] Even though the direct covalent linkage between porphyrin moieties is expected to form linear and rigid structure, the overall geometry of longer arrays (> 16) exhibit the curved structure due to the combinative summation of the dihedral and tilt angles between porphyrin moieties in the array. This feature is reminiscent of the case of tertiary or quaternary structure in proteins, and consequently increased fluorescence quenching sites in longer arrays. However, through host-guest interaction in **ZPHG**, the maintenance of linear structures seems to give rise to the reduction of shorter fluorescence decay components, leading to longer average fluorescence lifetimes compared to the corresponding **ZPH**. Thus, it should be noted that the fluorescence decay profiles in **ZPH** change from multiexponential to nearly single exponential decay with the guest molecule binding, indicating reduced conformational heterogeneity. In addition to the isotropic fluorescence decay, we measured the anisotropic fluorescence decays for the series of molecules in order to compare the rotational diffusion times (Φ_τ) with/without the guest molecules (Figure 4). Previously, the Φ_τ values were

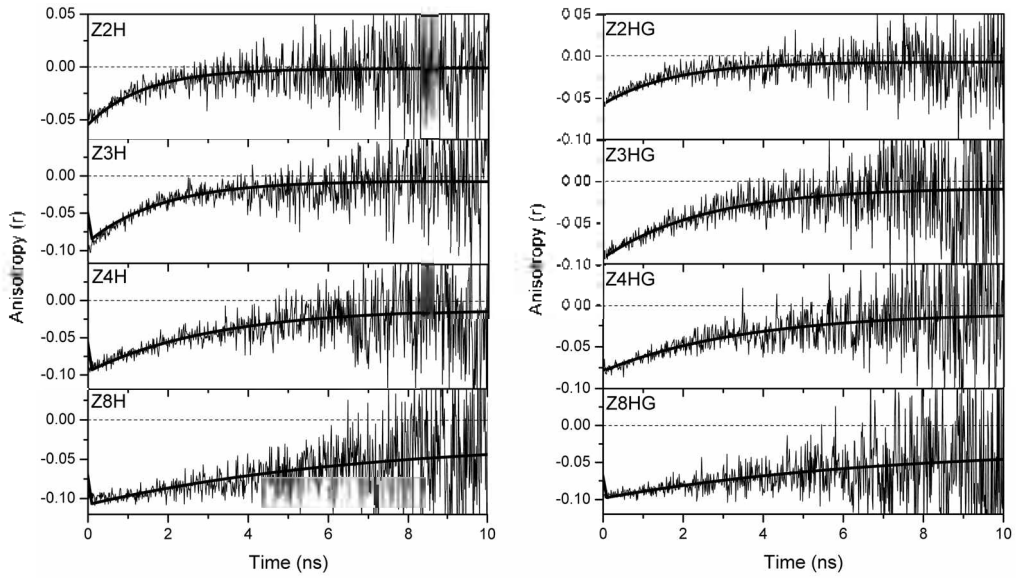

Figure 4. Fluorescence anisotropy decay profiles of **ZNH** and **ZNHG**, monitored at maxima fluorescence wavelengths, following the excitation with 400 nm femtosecond laser.

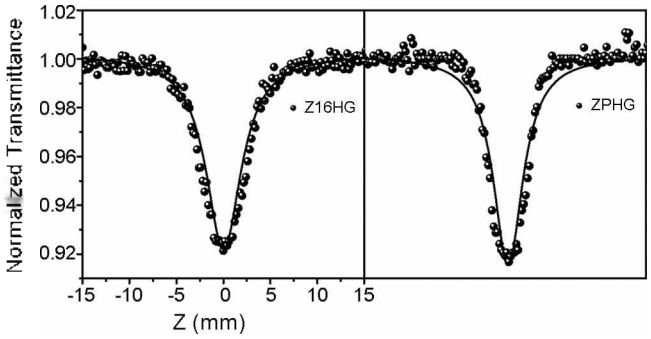

Figure 5. Open-aperture femtosecond Z-scan traces for **Z*16*HG** and **ZPHG**.

observed to increase, as the arrays become longer. In present case, the similar tendency in Φ_T was also observed as the arrays become longer in **Z*N*H**, and additionally, even slower rotational diffusion motion could be monitored in the **Z*N*HG** by enhanced molecular hydrodynamic volume, resulting from the rigid and linear molecular structures.

The increase of fluorescence quantum yields and the disappearance of fast decay component unequivocally support the structural change into helical form in **Z*N*HG** arrays. Additionally, referring to the previous reports, we can obtain information on delocalized π-conjugation pathway, excitonic coupling and molecular planarity from two-photon absorption (TPA) measurement.[14-16] In order to check the enhanced excitonic interactions accompanied by structural rigidity and delocalized π-conjugation, we have performed TPA measurement by an open aperture femtosecond Z-scan method with excitation at 800 nm, as shown in Figure 5. As indicated in Table 1, the TPA cross-section $\sigma^{(2)}$ values of **Z*N*H** remain intact with elongated molecular length, whereas that of **Z*N*HG** increases dramatically being consistent with the elongated π-conjugation length arising from reduced dihedral angle between porphyrin moieties. The TPA cross-section values become larger from **Z*2*HG** to **Z*4*HG** and then, as the arrays become even larger, the TPA cross-section values show a saturation behavior. This saturation behavior indicates that the regular and repetitive helical "pitch" in ZNHG with a complete one turn corresponds to 4-5 porphyrin monomeric units, reaching the maximum pi-conjugation along the porphyrin array **Z*N*HG**.

In summary, we have provided the spectroscopic evidences on the retrieved conformational homogeneity in **Z*N*HG** arrays by host-guest interaction; enhancement of fluorescence quantum yield and anisotropy,[17] and disappearance of fast fluorescence decay component. In addition, we were also able to observe the increased TPA cross-section values by enhanced excitonic interactions between porphyrin monomers in helical structures. Even though the direct microscopic evidence on conformational uniformity could not be detected in helical form, the overall spectroscopic observations consistently support that the negative effects due to conformational heterogeneity were mitigated through host-guest interaction. We expect that the current strategy of host-guest chemistry by hydrogen bonding can be exploited in designing homogeneous molecular electronic devices. Especially, in-depth nonlinear optical response in **Z*N*HG** is now under investigation, based on the enhanced TPA cross-section values with an anticipation to extend its applications in imaging or biomedical sensor.

Acknowledgements. This work was financially supported by the Star Faculty Program of the Ministry of Education and Human Resources Development of Korea (DK). EM and ZSY appreciate the fellowship of the BK 21 program from the Ministry of Education and Human Resources Development. DK thanks Professor Atsuhiro Osuka at University for his kind discussion and providing samples.

References

1. Kadish, K. M.; Smith, K. M.; Guilard, R. *The Porphyrin Handbook*; Academic Press: Boston, 2000.
2. Gust, D.; Moore, T. A.; Moore, A. L. *Acc. Chem. Res.* **2001**, *34*, 40.
3. Holten, D.; Bocian, D. F.; Lindsey, J. S. *Acc. Chem. Res.* **2002**, *35*, 57.
4. Kim, D.; Osuka, A. *J. Phys. Chem. A* **2003**, *107*, 8791.
5. Shimizu, S.; Osuka, A. *Eur. J. Inorg. Chem.* **2006**, 1319.
6. Aratani, N.; Osuka, A.; Kim, D.; Kim, Y. H.; Jeong, D. H. *Angew. Chem., Int. Ed.* **2000**, *39*, 1458.
7. Osuka, A.; Shimidzu, H. *Angew. Chem., Int. Ed. Engl.* **1997**, *36*, 135.
8. Kim, Y. H.; Jeong, D. H.; Kim, D.; Jeoung, S. C.; Cho, H. S.; Kim, S. K.; Aratani, N.; Osuka, A. *J. Am. Chem. Soc.* **2001**, *123*, 76.
9. Tsuda, A.; Osuka, A. *Science* **2001**, *293*, 79.
10. Aratani, N.; Takagi, A.; Yanagawa, Y.; Matsumoto, T.; Kawai, T.; Yoon, Z. S.; Kim, D.; Osuka, A. *Chem. Eur. J.* **2005**, *11*, 3389.
11. Ahn, T. K; Yoon, Z. S.; Hwang, I. W.; Lim, J. K.; Rhee, H.; Joo, T.; Sim, E.; Kim, S. K.; Aratani, N.; Osuka, A.; Kim, D. *J. Phys. Chem. B* **2005**, *109*, 11223.
12. Park, M.; Cho, S.; Yoon, Z. S.; Aratani, N.; Osuka, A.; Kim, D. *J. Am. Chem. Soc.* **2005**, *127*, 15201.
13. Ikeda, C.; Yoon, Z. S.; Park, M.; Inoue, H.; Kim, D.; Osuka, A. *J. Am. Soc. Chem.* **2005**, *127*, 534.
14. Ahn, T. K.; Kim, K. S.; Kim, D. Y.; Noh, S. B.; Aratani, N.; Ikeda, C.; Osuka, A.; Kim, D. *J. Am. Chem. Soc.* **2006**, *128*, 1700.
15. Kim, D. Y.; Ahn, T. K.; Kwon, J. H.; Kim, D.; Ikeue, T.; Aratani, N.; Osuka, A.; Shigeiwa, M.; Maeda, S. *J. Phys. Chem. A* **2005**, *109*, 2996.
16. Yoon, Z. S.; Kwon, J. H.; Yoon, M. C.; Koh, M. K.; Noh, S. B.; Sessler, J. L.; Lee, J. T.; Seidel, D.; Aguilar, A.; Shimizu, S.; Suzuki, M.; Osuka, A.; Kim, D. *J. Am. Chem. Soc.* **2006**, *128*, 14128.